

## Nuclear Magnetic Moment of $^{210}\text{Fr}$ : A Combined Theoretical and Experimental Approach

E. Gomez,<sup>1,\*</sup> S. Aubin,<sup>1,†</sup> L. A. Orozco,<sup>2</sup> G. D. Sprouse,<sup>1</sup> E. Iskrenova-Tchoukova,<sup>3</sup> and M. S. Safronova<sup>3</sup>

<sup>1</sup>Department of Physics and Astronomy, SUNY Stony Brook, Stony Brook, New York 11794-3800, USA

<sup>2</sup>Joint Quantum Institute, Department of Physics, University of Maryland, College Park, Maryland 20742-4111, USA

<sup>3</sup>Department of Physics and Astronomy, University of Delaware, Newark, Delaware 19716, USA

(Received 17 September 2007; published 2 May 2008)

We measure the hyperfine splitting of the  $9S_{1/2}$  level of  $^{210}\text{Fr}$ , and find a magnetic dipole hyperfine constant  $A = 622.25(36)$  MHz. The theoretical value, obtained using the relativistic all-order method from the electronic wave function at the nucleus, allows us to extract a nuclear magnetic moment of  $4.38(5)\mu_N$  for this isotope, which represents a factor of 2 improvement in precision over previous measurements. The same method can be applied to other rare isotopes and elements.

DOI: 10.1103/PhysRevLett.100.172502

PACS numbers: 21.10.Ky, 27.90.+b, 31.30.Gs, 32.10.Fn

The nuclear magnetic moment characterizes the magnetization of the nucleus with a single parameter. This fundamental quantity plays an important role in many atomic and nuclear processes including parity violating interactions. More specifically, the nuclear magnetic moment is necessary for extracting accurate information about the weak interaction in the nucleus [1] from atomic parity nonconservation (PNC) measurements [2]. Recent progress in *ab initio* calculations of the hyperfine constants of excited electronic states of alkali atoms [3] allows us to accurately extract the nuclear magnetic moment from a hyperfine splitting measurement. In the case of francium, the heaviest alkali, a measurement of the  $9S_{1/2}$  hyperfine splitting of  $^{210}\text{Fr}$  provides a hyperfine manifold with less dependence on electron correlations than the ground state for the extraction of the magnetic moment.

The interaction of an electron with the nuclear magnetic moment produces the hyperfine splitting of the electronic energy levels. More specifically, the  $9s$  level of  $^{210}\text{Fr}$  has two hyperfine levels with total angular momentum of  $F = 11/2$  and  $F = 13/2$  split by the interaction of the valence electron with angular momentum  $J = 1/2$  with the nuclear spin  $I = 6$ . The hyperfine level energy shift is  $E_{\text{hf}}/\hbar = AK/2$ , where  $K = F(F + 1) - I(I + 1) - J(J + 1)$  [4], and  $A$  is the magnetic dipole hyperfine constant given by the Fermi Segré formula [5]:

$$A = \frac{16\pi}{3h} \frac{\mu_0}{4\pi} g_I \mu_N \mu_B |\psi(0)|^2 \Xi, \quad (1)$$

where  $\mu_0$  is the magnetic constant,  $\mu_N$  is the nuclear magneton,  $\mu_B$  is the Bohr magneton,  $g_I$  is the nuclear  $g$  factor,  $\psi(0)$  is the wave function of the electron at the center of the nucleus, and  $\Xi$  includes the relativistic correction, the Breit-Rosenthal-Crawford-Schawlow [6–8] correction, and the Bohr-Weisskopf effect [9].

Equation (1) implies that a comparison with *ab initio* theory requires knowledge of the electronic wave function at the nucleus,  $\Xi$ , and  $g_I$ . All corrections are incorporated directly into the electronic wave function calculation including the nuclear structure. The electronic calculation

and a measurement of  $A$  from the hyperfine splitting can then be used to determine  $g_I$ . In the case of francium,  $g_I$  has been directly measured with an atomic beam magnetic resonance technique on the ground state with 2% precision in only one isotope:  $^{211}\text{Fr}$  [10]. We use the hyperfine splitting of an excited  $s$  level, since it is less sensitive to correlation corrections than the ground  $s$  level, despite its smaller value than the ground state. The  $g_I$  determination method presented in this letter provides a factor of 2 improvement in accuracy in francium and can also be applied to other elements.

The production, cooling and trapping of Fr online with the Superconducting LINAC at Stony Brook is described in Ref. [2]. Briefly, a 100 MeV beam of  $^{18}\text{O}$  ions from the accelerator impinges on a gold target to make  $^{210}\text{Fr}$ . We extract  $\sim 1 \times 10^6$  francium ions/s out of the gold and transport them about 15 m to a cold yttrium neutralizer where we accumulate the Fr atoms. We heat the neutralizer which releases neutral francium atoms into a dry-film coated vacuum glass, where we cool and trap  $10^4$ – $10^5$  atoms in steady state in a magneto-optical trap.

Figure 1 shows the energy levels of  $^{210}\text{Fr}$  relevant for trapping and the hyperfine splitting measurements. A titanium-sapphire (Ti:sapphire) laser at 718 nm provides cooling and trapping light near the cycling transition ( $7S_{1/2}$ ,  $F = 13/2 \rightarrow 7P_{3/2}$ ,  $F = 15/2$ ). A second Ti:sapphire laser at 817 nm repumps atoms that leak out of the cooling cycle via the  $7S_{1/2}$ ,  $F = 11/2 \rightarrow 7P_{1/2}$ ,  $F = 11/2$  transition.

We excite the  $9s$  level in a manner similar to that used for previous measurements of the atomic lifetimes of the  $9s$  and  $8p$  levels [11]. Atoms are moved out of the trap cycling transition with a depumping laser pulse ( $7S_{1/2}$ ,  $F = 13/2 \rightarrow 7P_{3/2}$ ,  $F = 13/2$ ) and into the  $7S_{1/2}$ ,  $F = 11/2$  level where a subsequent pulse from the repumper laser takes them to the  $7P_{1/2}$ ,  $F = 11/2$  level. From this last level, we excite atoms to the  $9s$  levels with a laser pulse (100–400 ns long) at 744 nm from a third Ti:sapphire laser which is turned off in 10 ns with an extinction ratio better

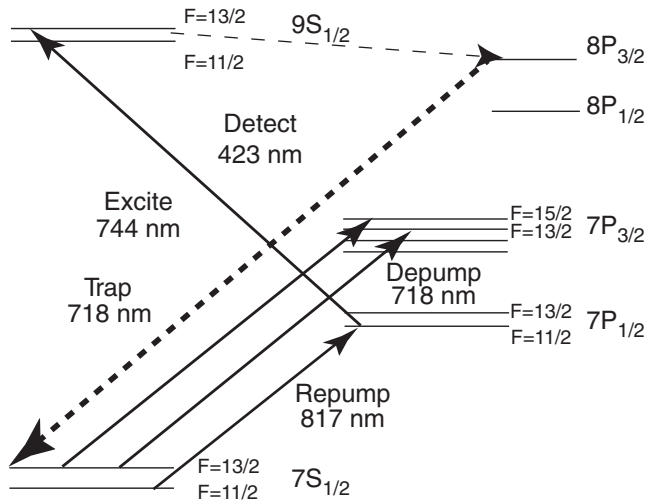


FIG. 1. Energy levels of Fr for trapping and  $9S_{1/2}$  hyperfine measurement.

than 400:1 by electro-optical and acousto-optical modulators. We scan the 744 nm excitation laser across the  $7P_{1/2}$   $F = 11/2 \rightarrow 9S_{1/2}$   $F = 11/2$  and  $7P_{1/2}$   $F = 11/2 \rightarrow 9S_{1/2}$   $F = 13/2$  transitions and record the fluorescence at 423 nm from the  $8P_{3/2}$  decay channel as a function of the optical excitation frequency (see Fig. 2,  $8P_{3/2} \rightarrow 7S_{1/2}$  decay channel).

We use a confocal temperature-stabilized Fabry-Perot cavity to lock all the lasers [12] and as a ruler in frequency space. The cavity resonances of a stabilized helium-neon laser indicate the free spectral range of the cavity at 633 nm. We measure the cavity free spectral range  $F_{\text{fsr}} = 299.78 \pm 0.03$  MHz in the vicinity of the  $7P_{1/2} \rightarrow 9S_{1/2}$  transition at 744 nm. We determine the hyperfine splitting  $f_{\text{HFS}}$  by measuring the frequency difference of the two transitions modulo  $F_{\text{fsr}}$ . The integer number of cavity free spectral ranges separating the two hyperfine levels is determined from wave meter readings.

We understand the shape of the resonances with a model based on a density matrix approach described in

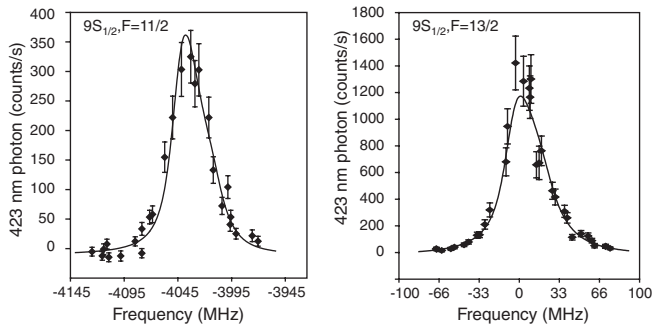


FIG. 2. Frequency scan of the  $9S_{1/2}$  state showing the two hyperfine resonances as labeled. The continuous lines are the model calculations. The frequency origin is centered around the  $7P_{1/2}$ ,  $F = 11/2 \rightarrow 9S_{1/2}$ ,  $F = 13/2$  transition.

Refs. [13,14]. The model calculates steady state populations in all the levels. The model includes a single  $7s$   $F = 11/2$  level, a single  $7P_{1/2}$  ( $F = 11/2$ ) level, and two  $9S_{1/2}$  levels. All other available levels enter only as decay paths and are included without hyperfine structure:  $7P_{3/2}$ ,  $8P_{1/2}$ ,  $8P_{3/2}$ ,  $6D_{3/2}$ ,  $6D_{5/2}$ . The model has two laser fields connecting the  $7s \rightarrow 7P_{1/2}$  at 817 nm and  $7P_{1/2} \rightarrow 9S_{1/2}$  at 744 nm. We solve it numerically for a given set of laser field parameters (detuning and intensity, assuming infinitely narrow laser linewidths), and for a given excitation path (which  $m_F$  levels participate in the excitation). We average the solution over the  $\pm 5.4$  MHz long term linewidths of the 817 and 744 nm excitation lasers. If there are several possible excitation paths (i.e. a spread of  $m_F$  levels are used), then this can show up as a broadening. The model incorporates the possibility of different excitation paths by solving the density matrix for each individual excitation path that has a corresponding ac Stark shift. Finally, we average over a range of laser intensities to account for the focusing of the excitation lasers.

The experimental data are fitted to the result of the model using a nonlinear least-squares fit (Marquardt-Levenberg). The model fits the individual  $9s$  resonances well (reduced  $\chi^2 \leq 1.7$ ). Figure 2 shows experimental data with the fit, including the amplitude as a parameter, applied separately to the two resonances. The observed line shapes are in agreement with the fitting model, which includes possible differential ac Stark shifts. The differential ac Stark shift is small and appears due to a slight detuning of the 817 nm laser from resonance.

The uncertainty in the measurement is dominated by the statistical error of  $\pm 1.89$  MHz on the fit. Other contributions are the cavity calibration ( $\pm 0.42$  MHz), the linearity of the cavity scan ( $\pm 0.28$  MHz), the differential Zeeman shift ( $\pm 0.87$  MHz), and differential Doppler shifts due to the pushing of the atoms by the excitation lasers ( $\pm 0.96$  MHz). We measure the hyperfine splitting of the  $9s$  level to be  $f_{\text{HFS}} = 4044.65 \pm 2.34$  MHz. This hyperfine splitting corresponds to a hyperfine magnetic dipole constant of  $A = 622.25 \pm 0.36$  MHz. The measurement has a fractional uncertainty of 0.06%. A direct wave meter measurement of the hyperfine splitting, consistent with the previous number, also gives the (center of gravity)  $7S_{1/2} \rightarrow 9S_{1/2}$  transition energy  $\Delta E = 25671.0153 \pm 0.0014$  cm $^{-1}$ , itself consistent with the location of the  $9S_{1/2}$ ,  $F = 13/2$  state in  $^{210}\text{Fr}$  [2].

Our high-precision calculation of the  $^{210}\text{Fr}$  nuclear magnetic values using a relativistic all-order method, includes all single, double, and partial triple (SDpT) excitations of the Dirac-Hartree-Fock wave function to all orders of perturbation theory [3]. The *ab initio* values of the hyperfine constants for the  $ns$  and  $np_{1/2}$  states of the alkali-metal atoms from Na to Cs obtained by this method agree with experiment to 1% or better [3]. We establish the accuracy of the determination of the  $^{210}\text{Fr}$  nuclear magnetic moment

TABLE I. Hyperfine magnetic dipole constants  $A$  for the  $ns$  states of  $^{133}\text{Cs}$  and  $^{210}\text{Fr}$  in MHz including the percentage contributions of the correlation correction and triple excitations.

	Cs	6s	7s	8s
DHF		1424	391.2	163.4
SD		2439	560.9	223.4
Final		2276	540.0	216.8
Correlation(%)		37.4	27.6	24.6
Triple excitations (%)		-7.2	-3.9	-3.1
Experiment		2298.157	545.90(9)	219.3(1)
Reference		[4]	[15]	[16]
Fr		7s	8s	9s
DHF		4762	1220	501.2
SD		7750	1632	639.1
Final		7277	1584	624.8
Correlation(%)		34.6	22.9	19.8
Triple excitations (%)		-6.5	-3.1	-2.3
Experiment		7195.1(9)	1577.8(23)	622.32(30)
Reference		[17]	[18]	Present Letter

using our calculation of the Cs hyperfine constants. Table I summarizes the calculations for Cs and Fr. We list lowest-order Dirac-Hartree-Fock results (DHF), all-order SD results which exclude all triple contributions, and our final SDpT results.

Since we use Cs as the benchmark test for the determination of the  $^{210}\text{Fr}$  nuclear magnetic moment, we only need to study the difference in the application of the SDpT method to Cs and Fr. To compare Cs and Fr cases, we also include the relative contribution of the correlation correction, defined as the difference of the final results and DHF values, relative to the final values as well as the relative contribution of the triple excitations, defined as the difference of the SDpT and SD values, relative to the final values. These comparisons show that Fr and Cs cases are very similar, as expected. As it was shown in Refs. [19–21], the inclusion of the effects of the triple excitations beyond the ones included in this work, as well as other higher-order effects, is significantly cancelled out by the nonlinear terms. Small differences in the relative contributions are most likely due to slightly different cancellations in the correlation correction terms in Cs and Fr cases.

We probe the effect of some of the omitted higher-order correlation corrections with a sensitivity analysis that uses a semiempirical scaling of the dominant contribution of the correlation correction [3]. The resulting relative correction, defined as the difference of the *ab initio* SDpT and scaled SDpT results, relative to *ab initio* results, is  $-1.5\%$  for  $A(7s)$  and  $-1.3\%$  for  $A(8s)$  for Cs. The corresponding values for Fr are  $-0.9\%$  and  $-0.5\%$  for  $A(8s)$  and  $A(9s)$ , respectively. We calculated the contributions of the valence nonlinear SD terms and found them to be relatively the same for the corresponding Cs and Fr  $ns$  states. The contribution of the core nonlinear terms, which may increase

from Cs to Fr, is substantially smaller than the contribution of the valence nonlinear terms [21].

The only other significant difference between the Cs and Fr calculations is the sensitivity of the theoretical hyperfine constant values to the nuclear magnetization distribution. Measurements of the hyperfine anomaly can give more information about the magnetization distribution [22]. It is expected that the Cs calculation will be much less sensitive to that effect than the Fr calculation. We model this magnetization distribution using the Fermi distribution with the same parameters as we use for the charge distribution. We use a Fermi half-density with  $c = 5.6748$  fm and  $c = 6.7241$  fm for Cs and Fr, respectively; the skin thickness parameter is taken to be 2.3 fm for both atoms. We study the dependence of the calculated hyperfine constants on  $c$  by conducting two additional calculations with  $c$  modified by 10% and 20% for both Cs and Fr. We find that all  $ns$  states are affected by the change in magnetization distribution in the same way. A 10% change in the values of  $c$  results in 0.4% change in the values of Fr  $ns$  hyperfine constants and 20% change in the values of  $c$  results in 0.8% change in all values. For Cs, 10% and 20% changes in  $c$  values result in 0.1% and 0.2% changes in the  $ns$  hyperfine constants, respectively. We note that our approach relies on the rough modeling of the Bohr-Weisskopf effect. Nevertheless, the comparison of our calculations with others [22–25] show that the discrepancy in the relevant Fr–Cs difference is below 1%. We investigate further the effect of the uncertainty in the nuclear magnetization distribution by conducting the same study on the  $7P_{1/2}$  levels of Fr. The effect of the magnetization distribution is 3 times smaller for the  $7P_{1/2}$  state than for the  $ns$  states, 0.13% for 10% change in  $c$ , while the total correlation effect is larger, 47%. The nuclear magnetic moment extracted from the  $7P_{1/2}$  value,  $4.33\mu_N$ , is within 1% of the value derived from the  $7s$  state.

Figure 3 shows the ratio of the extracted magnetic moment  $\mu_{\text{exp}}$ , based on the experimentally measured  $A_{\text{exp}}$  and the calculated  $A_{\text{cal}}$ , to the known magnetic moment  $\mu$  of the first three hyperfine splitting intervals in the  $s$  series of Na, K, Rb, and Cs, following the relation  $\mu_{\text{exp}}/\mu = A_{\text{exp}}/A_{\text{cal}}$ . Table I presents the calculated values of the hyperfine constants using a nuclear  $g$  factor of  $g_I = 0.737886$  for  $^{133}\text{Cs}$  and  $g_I = 0.733$  for  $^{210}\text{Fr}$ . The accuracy of the calculations is at worst 1% so that the extraction of the magnetic moment from the hyperfine measurement is dominated by the theoretical uncertainty and not the experimental one.

We extract the nuclear magnetic moment of  $^{210}\text{Fr}$  using:  $\mu_{\text{exp}} = \mu_{\text{th}}A_{\text{exp}}/A_{\text{cal}} = 4.38(5)\mu_N$  with the  $9s$  numbers of Table I, calculated with a trial value of the nuclear magnetic moment for  $^{210}\text{Fr}$  of  $\mu_{\text{th}} = 4.40\mu_N$ . The result, with an error of 1%, agrees with previous calculations of Dzuba *et al.* [26] and Vajed-Samii *et al.* [27] within their stated precisions. The numbers extracted from the  $8s$  and  $7s$

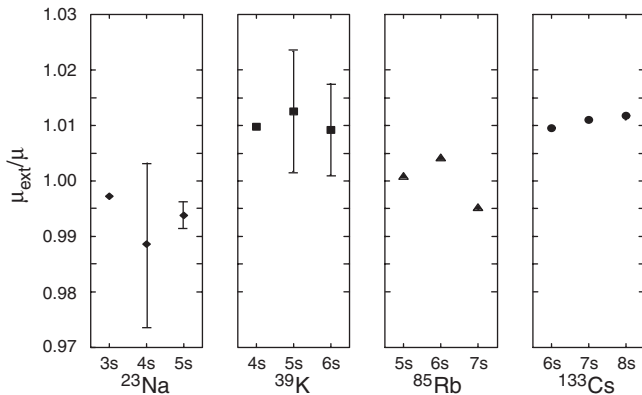


FIG. 3. Ratio of the extracted (measurement of the hyperfine splitting and theoretical calculation) to known magnetic moments (measured directly) for Na, K, Rb, and Cs for the lowest  $s$  levels. All error bars are due to the uncertainty of the measurements of the hyperfine  $A$  constant. The Na, K, and Rb calculations are from Ref. [3], and the Cs result is from the current work. The experimental values for Na and K come from Ref. [3] except the  $5s$  in Na [28], Rb:  $5s$  [4],  $6s$  [29], and  $7s$  [30], and for Cs  $6s$  [4],  $7s$  [15], and  $8s$  [16].

experiments and calculations are the same within our quoted error and all are consistent with the scaling of the measured magnetic moment of  $^{211}\text{Fr}$  [10].

The advances in *ab initio* calculations of the electronic wave functions in heavy alkali, particularly in Fr, have reached unprecedented accuracy and permit the extraction of the  $^{210}\text{Fr}$  nuclear magnetic moment based on a precise spectroscopic measurement of the  $9s$  hyperfine interval. The use of excited states reduces the size of correlation corrections and improves the accuracy of the calculation. This work is a novel approach to magnetic moment measurements in unstable isotopes.

This work has been supported by the NSF through No. PHY-0354956, No. PHY-0457078, and No. PHY-0098793. E.G. acknowledges support from CONACYT. The authors thank K. Gulyuz, B. Gutshow, R. Lefferts, and J. Sell for the operation of the Stony Brook LINAC. We thank V. Shabaev for his calculation of the Bohr-Weisskopf effect and helpful discussions.

\*Present address: Instituto de Física, Universidad Autónoma de San Luis Potosí, San Luis Potosí, Mexico.

†Present address: Department of Physics, College of William and Mary, Virginia 23187, USA.

- [1] E. Gomez, S. Aubin, G.D. Sprouse, L.A. Orozco, and D.P. DeMille, *Phys. Rev. A* **75**, 033418 (2007).
- [2] E. Gomez, L.A. Orozco, and G.D. Sprouse, *Rep. Prog. Phys.* **69**, 79 (2006).
- [3] M.S. Safronova, W.R. Johnson, and A. Derevianko, *Phys. Rev. A* **60**, 4476 (1999).

- [4] E. Arimondo, M. Inguscio, and P. Violino, *Rev. Mod. Phys.* **49**, 31 (1977).
- [5] L. Armstrong, Jr., *Theory of the Hyperfine Structure of Free Atoms* (Wiley-Interscience, New York, 1971), p. 137.
- [6] J.E. Rosenthal and G. Breit, *Phys. Rev.* **41**, 459 (1932).
- [7] M.F. Crawford and A.L. Schawlow, *Phys. Rev.* **76**, 1310 (1949).
- [8] H.J. Rosenberg and H.H. Stroke, *Phys. Rev. A* **5**, 1992 (1972).
- [9] A. Bohr and V.F. Weisskopf, *Phys. Rev.* **77**, 94 (1950).
- [10] C. Ekström, L. Robertsson, and A. Rosén, *Phys. Scr.* **34**, 624 (1986).
- [11] S. Aubin, E. Gomez, L.A. Orozco, and G.D. Sprouse, *Opt. Lett.* **28**, 2055 (2003); *Phys. Rev. A* **70**, 042504 (2004).
- [12] W.Z. Zhao, J.E. Simsarian, L.A. Orozco, and G.D. Sprouse, *Rev. Sci. Instrum.* **69**, 3737 (1998).
- [13] J.H. Marquardt, H.G. Robinson, and L. Hollberg, *J. Opt. Soc. Am. B* **13**, 1384 (1996).
- [14] J.M. Grossman, R.P. Filler, III, T.E. Mehlstäubler, L.A. Orozco, M.R. Pearson, G.D. Sprouse, and W.Z. Zhao, *Phys. Rev. A* **62**, 052507 (2000).
- [15] S.L. Gilbert, R.N. Watts, and C.E. Wieman, *Phys. Rev. A* **27**, 581 (1983).
- [16] P.P. Herrmann, J. Hoffnagle, A. Pedroni, N. Schlumpf, and A. Weis, *Opt. Commun.* **56**, 22 (1985).
- [17] A. Coc, C. Thibault, F. Touchard, H.T. Duong, P. Juncar, S. Liberman, J. Pinard, J. Lermé, J.L. Vialle, S. Büttgenbach, A.C. Mueller, A. Pesnelle, and (The ISOLDE Collaboration), *Phys. Lett. B* **163**, 66 (1985).
- [18] J.E. Simsarian, W.Z. Zhao, L.A. Orozco, and G.D. Sprouse, *Phys. Rev. A* **59**, 195 (1999).
- [19] S.G. Porsev and A. Derevianko, *Phys. Rev. A* **73**, 012501 (2006).
- [20] A. Derevianko and S.G. Porsev, *Eur. Phys. J. A* **32**, 517 (2007).
- [21] R. Pal, M.S. Safronova, W.R. Johnson, A. Derevianko, and S.G. Porsev, *Phys. Rev. A* **75**, 042515 (2007).
- [22] J.S. Grossman, L.A. Orozco, M.R. Pearson, J.E. Simsarian, G.D. Sprouse, and W.Z. Zhao, *Phys. Rev. Lett.* **83**, 935 (1999).
- [23] V.M. Shabaev, *J. Phys. B* **27**, 5825 (1994).
- [24] V.M. Shabaev, M. Tomaselli, T. Kühl, A.N. Artemyev, and V.A. Yerokhin, *Phys. Rev. A* **56**, 252 (1997).
- [25] V.M. Shabaev (private communication).
- [26] V.A. Dzuba, V.V. Flambaum, and O.P. Sushkov, *J. Phys. B* **17**, 1953 (1984).
- [27] Mina Vajed-Samii, J. Andriessen, B.P. Das, S.N. Ray, Taesul Lee, and T.P. Das, *Phys. Rev. Lett.* **48**, 1330 (1982); **49**, 1466 (1982); **49**, 1800 (1982).
- [28] L.G. Marcassa, S.R. Muniz, G.D. Telles, S.C. Zilio, and V.S. Bagnato, *Opt. Commun.* **155**, 38 (1998).
- [29] A. Pérez Galván, E. Gomez, F.J. Baumer, A.D. Lange, Y. Zhao, G.D. Sprouse, and L.A. Orozco, *Phys. Lett. B* **655**, 114 (2007).
- [30] E. Gomez, S. Aubin, L.A. Orozco, and G.D. Sprouse, *J. Opt. Soc. Am. B* **21**, 2058 (2004).